

MODELING AND BEHAVIOR OF NONLINEAR STATIC INSTABILITY OF LONG-SPAN CABLE-STAYED BRIDGES UNDER GRAVITY AND WIND LOADS

Virote BOONYAPINYO, Hitoshi YAMADA and Toshio MIYATA
Members, Yokohama National University

1. INTRODUCTION: When a cable-stayed bridge has a long span over 500 meters, static stability of the whole bridge increases its importance in design because of increases in: 1) the compressive forces in the towers and deck under gravity load, and 2) the wind load acting on the bridge. Under the wind effects, the long-span bridge is subjected to large, displacement-dependent wind loads of three components, i.e., a drag force, a lift force and a pitching moment. Moreover, the long-span bridge exhibits geometric nonlinearity due to beam-column effect, nonlinear behavior of cable, and bridge geometry change. Previous research on the static stability of this type of bridge has generally been based on the linear model, i.e., the linear bending buckling analysis under gravity load, linear lateral-torsional buckling and linear torsional divergence analyses under wind load. Now with the increase in the span length of this type of bridge, it is imperative to investigate the nonlinear buckling behavior. In this study, modeling and behavior of nonlinear static instability under gravity and displacement-dependent wind loads are presented by finite element method.

2. MODELING OF CABLE-STAYED BRIDGES: A cable-stayed bridge is idealized by a three-dimensional finite-element model. The tower and deck elements are idealized by a beam-column element. The nonlinear stiffness and various elastic instabilities, such as bending, torsional, and lateral-torsional bucklings are considered through the use of the geometric stiffness matrix of beam-columns augmenting the elastic stiffness matrix of beams¹⁻²⁾. The nonlinear behavior of cables due to the cable sag is considered through the use of the equivalent elastic stiffness of the cable as an equivalent straight chord element. In addition, the large nodal displacements of the stay cable are considered through the use of the geometric stiffness matrix of three-dimensional trusses augmenting the equivalent elastic stiffness matrix of cables.

3. MODELING OF NONLINEAR INSTABILITY

(1) Instability Under Gravity Load: Modeling of nonlinear instability under gravity load is based on the linearized incremental approach, together with the automatic selection of load increments. The linearized eigenvalue problem for the j^{th} step is written as:

$$[\mathbf{K}_e(u_{j-1}, \sigma_{j-1}) + \mathbf{K}_g(u_{j-1}, \sigma_{j-1})] \Delta \mathbf{U}_j = 0 \quad (1)$$

where \mathbf{K}_e and \mathbf{K}_g are the structural elastic and geometric stiffness matrices, respectively, $\Delta \mathbf{U}_j$ is the incremental displacement vector. The predicted instability load is $\mathbf{F}_{cr} = \mathbf{F}_{j-1} + \Delta \lambda \Delta \mathbf{F}_j$. At convergence, $\Delta \lambda = 0$ and $\mathbf{F}_{cr} = \mathbf{F}_{j-1}$.

(2) Instability Under Displacement-Dependent Wind Load: Modeling of nonlinear lateral-torsional buckling under displacement-dependent wind load is based on the incremental-iterative approach, together with the automatic selection of trial critical wind velocity. The linearized incremental equilibrium equation for j^{th} iteration is written as (Fig. 1)

$$\left. \begin{aligned} & [\mathbf{K}_e(u_{j-1}, \sigma_{j-1}) + \mathbf{K}_g^{G+W}(u_{j-1}, \sigma_{j-1})] \Delta \mathbf{U}_j \\ & = \mathbf{F}_j(F_X(\alpha_j), F_Y(\alpha_j), M_Z(\alpha_j)) \\ & - \mathbf{F}_{j-1}(F_X(\alpha_{j-1}), F_Y(\alpha_{j-1}), M_Z(\alpha_{j-1})) \end{aligned} \right\} \quad (2)$$

where

$$\left. \begin{aligned} F_X(\alpha) &= \frac{1}{2} \rho V_r^2 A_n C_X(\alpha) \\ F_Y(\alpha) &= \frac{1}{2} \rho V_r^2 B C_Y(\alpha) \\ M_Z(\alpha) &= \frac{1}{2} \rho V_r^2 B^2 C_Z(\alpha) \end{aligned} \right\} \quad (3-5)$$

In Eqs. (2)-(5), superscripts G and W mean gravity and wind loads, respectively; \mathbf{F}_j and \mathbf{F}_{j-1} are the displacement-dependent wind load vectors based on the current and preceding wind angles of attack, respectively; F_X , F_Y and M_Z are, respectively, the drag force, lift force, and pitching moment in the bridge axes; C_X , C_Y , and C_Z are, respectively, the drag, lift and pitching moment coefficients in the bridge axes; V_r is the relative (horizontal component) wind velocity; ρ is the air density; B is the deck width; A_n is the vertical projected area of deck; α is the effective wind angles of attack consisting of the torsional displacement of deck θ and the wind angle of incidence α_0 . The above process will converge for any given wind velocity less than the critical wind velocity.

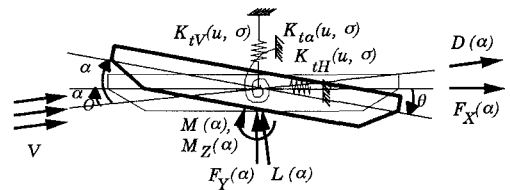


Fig. 1 Torsional displacement of a bridge deck and displacement-dependent wind load in wind and bridge axes

4. BEHAVIOR OF NONLINEAR INSTABILITY: The proposed modeling of nonlinear instability was applied to a long-span cable-stayed bridge with a center span length of 1000 meters during erection and on the completion (Fig. 2). The geometric nonlinearity in the long-span bridge results in significant reduction of the buckling load factor, compared with the linearized buckling analysis (Fig. 3). When all sources of geometric nonlinearity are considered, the bridge first exhibits the *hardening* structural behavior at the beginning of the incremental loads, and then the bridge becomes *softening* structural behavior as the applied load approaches the buckling load (Fig. 3).

The nonlinear lateral-torsional buckling analysis under the three-component displacement-dependent wind loads also results in significant reduction of the critical wind velocity (Fig. 4), compared with: (1) the linearized buckling analysis under the effect of initial wind forces, and (2) the torsional divergence analysis under the effect of pitching moment only. The reasons of such a reduction of the critical wind velocity are the considerations of: (a) the increase of the three-components of the wind loads due to the torsional displacements of the deck, and (b) the relaxation of the elastic stiffness of the cables due to the effects of lift forces and pitching moments. The positive angle of incidence significantly reduces the critical wind velocity (Fig. 5). The half-span bridge during erection is much more susceptible to the lateral-torsional buckling than the completed bridge (also Fig. 5).

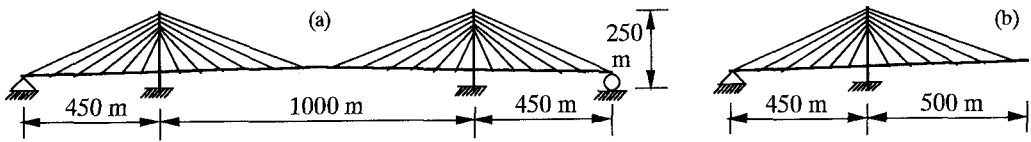


Fig. 2 Modeling of studied bridges: (a) a completed bridge, (b) a half-span bridge during erection

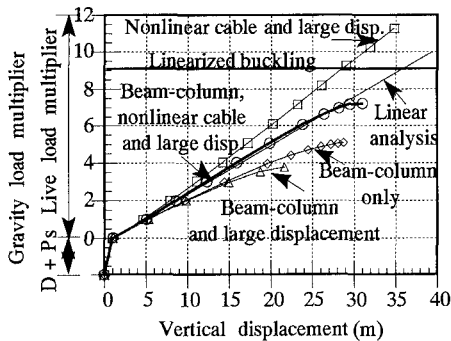


Fig. 3 Nonlinear load-displacement behavior at mid-span of a completed bridge using various sources of nonlinearity

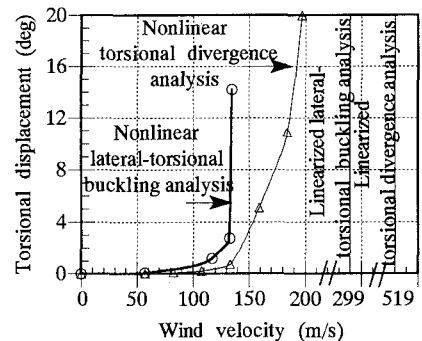


Fig. 4 Torsional behavior at mid-span of a completed bridge using various instability analysis types

5. CONCLUSIONS: The proposed, nonlinear instability modeling results in significant reduction of the instability load, compared with the linear one. Therefore, for long-span cable-stayed bridges, the static instability analysis should include the geometric nonlinearity as well as the three-component displacement-dependent wind loads to assure the adequacy of the total analysis. With regard to the static instability analysis, the cable-stayed bridge with the center span length of 1000 meters presents no serious problem and accordingly can be a realistic solution.

6. REFERENCES: 1) Yang, Y. B., and McGuir, W., "Stiffness Matrix for Geometric Nonlinear Analysis, and Joint Rotation and Geometric Nonlinear Analysis," *J. of Structural Engineering*, ASCE, Vol. 112(4), pp. 853-905, 1986. 2) Boonyapinyo, V., Yamada, M. and Miyata, T., "Nonlinear Buckling Instability Analysis of Long-Span Cable-Stayed Bridges under Displacement-Dependent Wind Load," *J. of Structural Engineering*, JSCE, Vol. 39A, pp. 923-936, March, 1993.

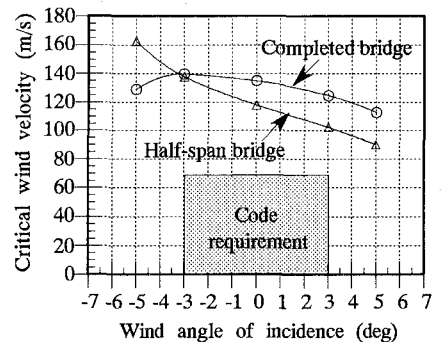


Fig. 5 Critical wind velocities of completed and half-span bridges for various wind angles of incidence